Virus Evolution, 2015, 1(1): vev008

doi: 10.1093/ve/vev008
Research article

Experimental evolution of an RNA virus in cells with innate immunity defects

Pablo Hernández-Alonso,† Raquel Garijo,† José M. Cuevas, and Rafael Sanjuán*,‡

Instituto Cavanilles de Biodiversidad y Biología Evolutiva and Departament de Genètica, Universitat de València, Paterna 46980, Spain

*Corresponding author: E-mail: rafael.sanjuan@uv.es
†These authors contributed equally to this work.
‡http://orcid.org/0000-0002-1844-545X

Abstract

Experimental evolution studies have shown that RNA viruses respond rapidly to directional selection and thus can adapt efficiently to changes in host cell tropism, antiviral drugs, or other imposed selective pressures. However, the evolution of RNA viruses under relaxed selection has been less extensively explored. Here, we evolved vesicular stomatitis virus in mouse embryonic fibroblasts knocked-out for PKR, a protein with a central role in antiviral innate immunity. Vesicular stomatitis virus adapted to PKR-negative mouse embryonic fibroblasts in a gene-specific manner, since the evolved viruses exhibited little or no fitness improvement in PKR-positive cells. Full-length sequencing revealed the presence of multiple parallel nucleotide substitutions arising in independent evolution lines. However, site-directed mutagenesis showed that the effects of these substitutions were not PKR dependent. In contrast, we found evidence for sign epistasis, such that a given substitution which was positively selected was strongly deleterious when tested as a single mutation. Our results suggest that virus evolution in cells with specific innate immunity defects may drive viral specialization. However, this process is not deterministic at the molecular level, probably because the fixation of mutations which are tolerated under a relaxed selection regime is governed mainly by random genetic drift.

Key words: experimental evolution, vesicular stomatitis virus, PKR, parallel evolution, epistasis, attenuation.

1 Introduction

Experimental evolution has been used to investigate drug resistance, pathogenesis, disease emergence, and other important topics in virology, as well as aid vaccine development. For instance, selection experiments in cell cultures can help to predict the emergence of drug-resistance mutations and their fitness costs in medically relevant viruses such as HIV-1, hepatitis C virus, and influenza virus (Koev and Kati 2008; Cahn and Wainberg 2010; Robinson et al. 2011; Triana-Baltzer et al. 2011; Wainberg, Mesplede, and Quashie 2012). In the context of viral emergence, experimental evolution has been used to study the selective constraints acting on host radiation (Turner and Elena 2000), the relationship between ecological specialization and host-shift risk (Turner et al. 2010), and the effects of host alternation on the adaptability and genetic diversity of vector-borne viruses (Coffey and Vignuzzi 2011; Ciota et al. 2014). Viral evolution in the laboratory has been particularly useful for the development of live attenuated vaccines. The pioneer procedures used for creating the first oral polio vaccines in the 1950s involved serial transfers in non-human hosts, plaque-to-plaque transfers, and viral propagation at low temperatures (Martin and Minor 2002). Similar techniques were used for the development of vaccines against measles, mumps, and yellow fever (Minor 2015). In these experiments, several evolutionary pro-

cesses were probably involved in viral attenuation. First, serial transfers in alternate host cells often lead to fitness losses in the original host, because mutations that are selectively advantageous in a given environment tend to be costly in alternate environments (Turner et al. 2000; Duffy, Turner, and Burch 2006; Buckling et al. 2009). Second, plaque-to-plaque transfers typically promote the accumulation of deleterious mutations through random genetic drift (Chao 1990; Duarte et al. 1992; de la Iglesia and Elena 2007). Finally, relaxed selection in permissive environments should favor the accumulation of conditionally deleterious mutations.

However, most of the above studies were designed with little knowledge of the molecular and cellular pathways involved. Here, we sought to take a more gene-based approach to the experimental evolution of viral attenuation. To explore this, we adapted a model virus to a permissive cellular environment by knocking-out the double-stranded RNA (dsRNA)-dependent protein kinase PKR, a major component of the innate immune response against viruses. PKR is induced by type-I interferons and is directly activated by viral dsRNA present in the cytoplasm. The best-known anti-viral effect of PKR is exerted through phosphorylation of the eukaryotic translation initiation factor 2, which induces translational shutoff, but PKR mediates additional antiviral responses through its effects on protein phosphorylation, mRNA stability, and apoptosis (García, Meurs, and Esteban 2007; Pindel and Sadler 2011; Dabo and Meurs 2012; Munir and Berg 2013). The ability to suppress PKR activity and other innate immune responses is thus a major determinant of viral fitness and has promoted the evolution of multiple immune evasion mechanisms including inhibition of upstream pathogen sensors such as RIG-I, signal transducers, and effector antiviral proteins such as PKR (Bowie and Unterholzner 2008; Versteeg and Garcia-Sastre 2010; Hoffmann, Schneider, and Rice 2015). Therefore, we reasoned that relaxation of the selective pressure exerted by PKR should create a permissive environment that may promote the fixation of effectively neutral mutations usually not tolerated in cells with intact innate immunity. In addition to this 'drift hypothesis', other processes may contribute to promoting viral attenuation. For instance, some mutations may be selectively advantageous in PKR negative but neutral or deleterious in normal cells (selection hypothesis).

To test these ideas, we chose vesicular stomatitis virus (VSV) as model system, a prototypic non-segmented negative-stranded RNA virus of the family Rhabdoviridae. VSV can be easily propagated in most mammalian cells and is highly sensitive to PKR, as illustrated by the fact that the viral lethal dose is reduced by orders of magnitude in PKR-deficient mice, although this effect is more modest in cell cultures (Balachandran et al. 2000; Stojdl et al. 2000). We found that VSV readily adapted to PKR-deficient mouse embryonic fibroblasts (MEFs), and that this adaptation was PKR-dependent, since the evolved viruses exhibited no fitness gains in PKR-positive MEFs. We also sought to investigate the genetic basis of this adaptation by sequencing the full viral genome. This revealed several parallel substitutions in the evolved lines, and we demonstrate the beneficial fitness effects of these substitutions by site-directed mutagenesis. However, most parallel substitutions were also beneficial in PKR-positive MEFs and other cell types and thus were not responsible for PKR-dependent changes in fitness. Therefore, some of the non-parallel substitutions may be deleterious in PKR-positive cells and counteract the generally beneficial effects of parallel substitutions. Consequently, in the absence of PKR, relaxed selection may have allowed for the fixation of mutations with conditionally deleterious effects in cells with normal antiviral immunity, but these mutations did not reach fixation in a deterministic or repeatable manner. Hence, the genetic data lend support to the drift hypothesis for viral attenuation. We also found that one of the parallel substitutions appearing in multiple evolution lines was strongly deleterious when assayed as a single mutation, underscoring the importance of epistasis for adaptation. Collectively, our results suggest that experimental evolution in cells with gene-specific defects in innate immunity may drive viral attenuation, but that this process can be obscured by the appearance of generally beneficial mutations, genetic drift, and by gene-by-gene interactions.

2 Methods

2.1 Virus and cell culturing

VSV was recovered from a cDNA clone, originally created by Whelan et al. (Whelan et al. 1995), by transfecting BHK-21 cells as previously described (Sanjuán, Moya, and Elena 2004). This virus was used as the founder of the evolution experiment (T0). Primary MEFs derived from *pkr* −/− or wild-type C57BL6 mice were isolated as previously described (Palmero and Serrano 2001) and were provided by Dr Carmen Rivas (Universidad de Santiago de Compostela, Spain). Cells were cultured in Dulbeco's modified Eagle's Medium (Invitrogen) supplemented with 10 per cent fetal bovine serum (Invitrogen) at 37°C under 95 per cent humidity and 5 per cent CO_2, and immortalized by serial passaging. The absence of the *pkr* gene was verified by polymerase chain reaction (PCR).

2.2 Experimental evolution

MEF monolayers containing approximately 10^5 cells were inoculated with 10^4 particle forming units (PFU) and incubated for 24 h, the time required to reach a titer plateau of approximately 5×10^7 PFU/ml, as determined by growth curves. The supernatants were titrated after each passage by the standard plaque assay in baby hamster kidney (BHK-21) cells (ATCC) and diluted as required to infect fresh cells with a constant number of PFUs throughout the course of the experiment. Assuming a yield of approximately 1,000 PFU/cell, the estimated number of viral generations (i.e., infection cycles) per passage is $\ln(5 \times 10^7/10^4)/\ln 10^3 = 1.23$ (Miralles, Moya, and Elena 2000).

2.3 Growth curves and model fitting

MEF monolayers containing approximately 10^5 cells were inoculated with 10^4 PFU, and small volumes were sampled at the indicated times and titrated by the standard plaque assay. A logistic growth model with viral decay of the form $N_t = \frac{N_{max}}{1+e^{c-rt}} e^{-dt}$ was fit to the data, where N_t is the observed titer, r the exponential growth rate, N_{max} the maximal viral yield in the absence of degradation, c sets the initial conditions, and d is the viral decay (degradation) rate. The model was fit to the data by the least-squares method for each experimental replicate separately. We obtained r^2 values higher than 0.95 in all cases and higher than 0.99 in most cases.

2.4 Fitness assays

MEF monolayers containing approximately 10^5 cells were inoculated with 10^4 PFU of the assayed virus (evolved or T0) and a common competitor which was isogenic to the T0 virus except for a single-nucleotide replacement (C3853A) in the surface glycoprotein gene G which controls sensitivity to a monoclonal

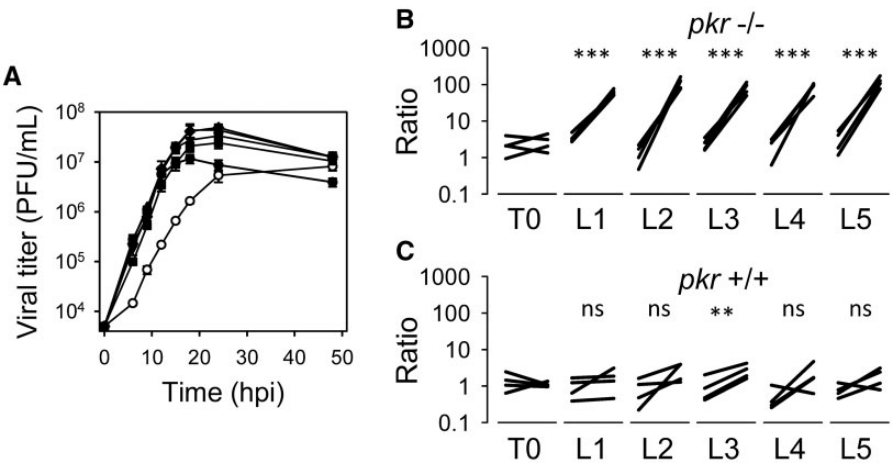

Figure 1. VSV adaptation to pkr-/- MEFs. (A) Growth curve of the five evolved lines (filled circles) and the founder (T0) virus (open circles). Each line was assayed in triplicate. Error bars indicate the standard error of the mean. (B) Competition assays of the T0 and evolved viruses against a common, phenotypically marked competitor in *pkr* -/- MEFs. Each line represents the change in the ratio of the assayed virus to the common competitor after a single 24 h transfer and corresponds to one replicate assay. Four replicates were performed for each competition. (C) Competition assays in *pkr* +/+ MEFs were performed in the same way as in (B).

Table 1. Growth parameters of the five lines adapted to PKR-negative MEFs.

Line	Growth rate (h^{-1})	Maximal yield (PFU/ml $\times 10^{-7}$)	Decay rate (h^{-1})
T0	0.38 ± 0.02	1.27 ± 0.21	0.02 ± 0.01
L1	$0.66 \pm 0.00^{***}$	1.03 ± 0.08	0.03 ± 0.01
L2	$0.64 \pm 0.00^{***}$	4.48 ± 1.25	0.04 ± 0.02
L3	$0.63 \pm 0.02^{***}$	$3.33 \pm 0.91^{*}$	0.03 ± 0.01
L4	$0.57 \pm 0.02^{***}$	$2.61 \pm 0.52^{*}$	0.04 ± 0.01
L5	$0.63 \pm 0.03^{***}$	$5.09 \pm 0.93^{*}$	0.05 ± 0.02

$^{*}P < 0.05$; $^{***}P < 0.001$ (t-test against T0).

antibody (Sanjuán, Moya, and Elena 2004). The proportion of each competitor at inoculation and after a single 24 h transfer was determined by titrating the mix in the presence and in the absence of antibody in BHK-21 cells. Fitness was calculated as $W = R_{24}/R_0$, where R denotes the titer ratio of the assayed virus relative to the common competitor at inoculation ($T0$) and after 24 h.

2.5 Sequencing

Viral RNA was extracted from virus supernatants using the NucleoSpin RNA Virus kit (Macherey-Nagel), reverse transcribed with AccuScript (Agilent Technologies), and used for PCR amplification. The viral genome was amplified using eight different, overlapping, primer pairs (sequence available upon request). PCRs were column purified and used for Sanger sequencing. Chromatograms were analyzed with the Staden package (http://staden.sourceforge.net).

2.6 Site-directed mutagenesis

Mutations were introduced using a pair of self-complementary primers carrying the desired change. The cDNA clone was amplified for eighteen cycles using the high-fidelity Phusion DNA polymerase (New England Biolabs). To remove template DNA, amplification products were digested with DpnI (New England Biolabs), which selectively cuts methylated GATC sites. Products were used for transforming competent *Escherichia coli* cells by the rubidium chloride heat-shock method. Plasmid DNA was then purified using the Nucleospin Plasmid purification kit (Macherey-Nagel) and used for transfecting BHK-21 cells as previously described (Whelan et al. 1995; Sanjuán, Moya, and Elena 2004). Briefly, young 90 per cent confluent BHK-21 cells were infected with a recombinant vaccinia virus expressing T7 RNA polymerase and then co-transfected with the full-length VSV cDNA clone and three helper plasmids encoding the P, L, and N proteins. Transfections were done using Lipofectamine LTX (Life Technologies), following manufacturer's instructions. After 6 h, 25 μg/ml 1-β-D-arabinofuranosylcytosine was added to inhibit vaccinia replication. After 3–4 days, supernatants were tested for the presence of infectious VSV particles by the standard plaque assay, vaccinia virus was removed by filtration, and one additional VSV infection cycle was performed to reach sufficient titer.

2.7 RNA structure prediction

The predicted minimum free energy of the trailer sequence was obtained using the RNAfold server available online (rna.tbi.univie.ac.at/cgi-bin/RNAfold.cgi) with default parameter options.

3 Results

VSV was recovered from an infectious cDNA clone and used for propagating five independent lines (L1–L5) for forty transfers in *pkr*−/− MEFs, which corresponds to approximately fifty generations (infection cycles) of viral evolution. To assess adaptation, we performed growth curves of the founder virus (T0) and each evolved line (Fig. 1A). Fit of a logistic growth model with viral decay showed that the exponential growth rate increased significantly in each of the lines (from $0.38\,h^{-1}$ in T0 to $0.57–0.66\,h^{-1}$; Table 1). This change represents a strong fitness gain, since the amount of viral progeny produced in 10 h of growth (∼one infection cycle) (Cuevas, Moya, and Sanjuán 2005) was approximately 10-fold higher for the evolved lines than for the founder virus. The maximal viral yield also tended to increase (from two- to fourfold; Table 1) except in line L1, although the data showed higher variance, and differences were thus less significant. Finally, we found no evidence for changes in particle stability, as inferred by viral decay rates. We therefore conclude that VSV adapted to PKR-negative cells mainly by increasing its short-term growth rate.

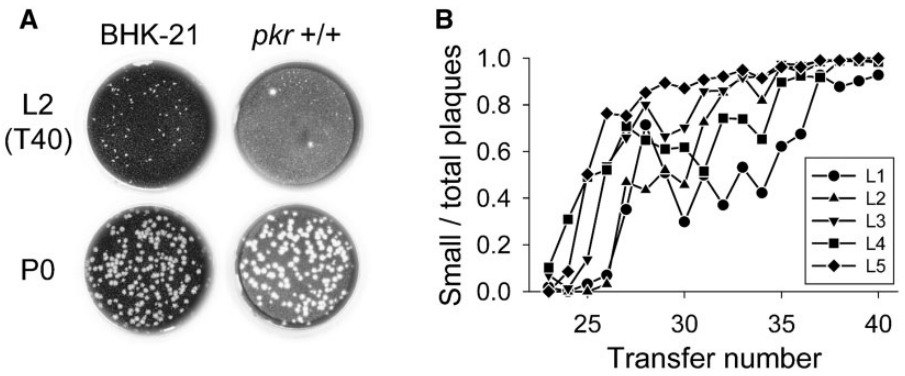

Figure 2. Serial transfers in *pkr* -/- MEFs select for a small-plaque phenotype in PKR-positive cells. (A) Plaque assays of the T0 virus and line L2 (transfer 40) in BHK-21 cells and in *pkr* +/+ MEFs. (B) Fixation of the small-plaque phenotype (assayed in BHK-21 cells) during evolution. Approximately 100 plaques from a single plaque assay were counted to determine the small/total plaque ratio. Small plaques were not observed before passage 22 and reached quasi-fixation in all lines except L1 by transfer 35.

Table 2. Genetic changes detected in the five lines adapted to PKR-negative MEFs.

Genome	Gene	Residue	L1	L2	L3	L4	L5
C1282U	N	None	–	–	–	+	–
C2649U	M	H134Y	–	–	+	–	–
G2686A	M	G146E	–	+	–	–	+
U3030C	Inter	None	+	–	–	–	–
G3351A	G	E92K	–	+	+	–	+
A3460C	G	Q128P	+	–	–	+	–
G3837A	G	E254K	–	+	+	+	+
C4180A	G	T368K	+	–	–	–	–
G4182A	G	E369K	+	–	–	–	–
U4397C	G	None	–	–	+	–	–
A4730G	Inter	None	–	–	–	+	–
G5557A	L	None	+	–	–	–	–
A5700U	L	D323V	+	–	–	–	–
A6931G	L	None	–	–	+	–	–
U7369C	L	None	–	–	+	–	–
U7522C	L	None	–	–	+	–	–
G7591A	L	None	+	–	–	–	–
A8320G	L	None	+	–	–	–	–
A8679C	L	D1316A	–	+	–	–	+
C10224U	L	T1831M	+	+	–	+	–
C10282A	L	None	–	–	+	–	–
A11090G	Trailer	None	–	+	–	–	+

To further test for fitness changes, we also performed head-to-head competition assays against a phenotypically marked competitor isogenic to the T0 virus. Fitness (W), measured as the change in titer ratio relative to the common competitor after a single transfer, was >10 times higher for the evolved lines ($W = 18.5$, $W = 38.2$, $W = 17.5$, $W = 13.0$, $W = 15.2$ for L1–L5, respectively; *t*-test of logW against zero: $P < 0.001$ for all lines) than for the T0 virus ($W = 1.15$; $P = 0.132$; Fig. 1B). To ascertain whether the observed fitness changes were specific to PKR-negative cells, we performed identical competition assays in *pkr* +/+ MEFs. Lines L1, L2, L4, and L5 showed marginally significant increases in fitness (*t*-test of logW against zero: $0.134 > P > 0.057$), whereas L3 showed a more marked increase ($W = 6.22$; $P = 0.002$) but still less pronounced than in *pkr* −/− cells (Fig. 1C).

Therefore, viral adaptation was PKR dependent. We also noticed that, throughout the course of the evolution experiment, there was a strong reduction in plaque size in BHK-21 cells. Although *pkr*−/− MEF monolayers did not reach enough density to perform plaque assays, we verified the reproducibility of the small-plaque phenotype in *pkr* +/+ MEFs (Fig. 2A). The population frequency of this plaque phenotype gradually increased until reaching fixation (>98%) in all lines except L1, in which the population was still polymorphic by passage 40 although small plaques were highly abundant (~90%; Fig. 2B). Therefore, adaptation to *pkr* −/− cells was accompanied by a clear reduction in plaque size in PKR-positive cells.

To investigate the genetic basis of the observed changes in fitness and plaque size, we sequenced each of the evolved lines. In total, we found 22 nucleotide substitutions compared with the T0 virus, of which seven (G2686A, G3351A, A3460C, G3837A, A8679C, C10224U, and A11090G) appeared in two or more lines and thus represent cases of parallel evolution (Table 2). Previous work with VSV (Cuevas, Elena, and Moya 2002; Novella and Ebendick-Corpus 2004; Novella et al. 2004, 2010; Remold, Rambaut, and Turner 2008; Cuevas, Moya, and Sanjuán 2009) and several other viruses (Cunningham et al. 1997; Rico et al. 2006; Agudelo-Romero, de la Iglesia, and Elena 2008; Betancourt 2009; Wichman and Brown 2010; Borderia et al. 2015) has suggested that parallel substitutions tend to be selectively advantageous mutations, although their effects have not usually been assayed directly. Six of these changes were non-synonymous, and most produced non-conservative amino acid replacements, thus further suggesting a significant fitness effect. We noticed that the G3837A substitution occurred in lines L2–L5, all of which showed a small-plaque phenotype in *pkr* +/+ cells but that it was absent from L1 in which this phenotype was not fixed, thus suggesting that this mutation was responsible for small plaque formation.

To dissect the effects of the parallel substitutions on fitness and plaque size, we introduced them individually into the parental cDNA clone by site-directed mutagenesis and transfected BHK-21 cells to recover mutant viruses. We successfully recovered all single mutants except C10224U. As predicted, the G3837A mutation produced a small-plaque phenotype but, immediately after recovery, normal-plaque revertants were observed at 3, 3, 4, 40, and 90% population frequencies in five independent transfections, indicating that the G3837A mutation was severely deleterious in BHK-21 cells. This was confirmed by competition assays in *pkr* +/+ MEFs, which yielded an extremely low fitness value of $W = 0.081$ (*t*-test of log W against zero: $P = 0.003$). We then performed competition assays for each of the six single mutants in *pkr* −/− cells. Beneficial fitness

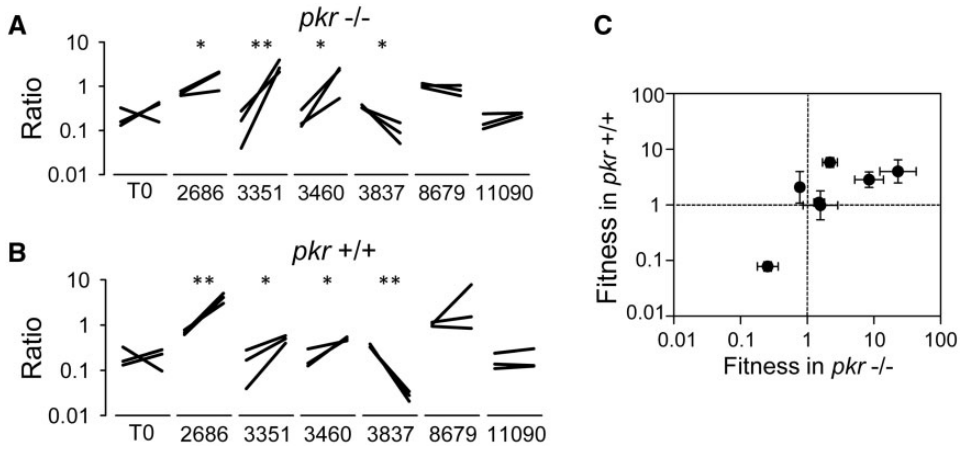

Figure 3. Individual fitness effects of parallel substitutions. (A) Competition assays of the T0 and single mutants against a common, phenotypically marked competitor in *pkr* -/- MEFs. Each line represents the change in the ratio of the assayed virus to the common competitor after a single 24 h transfer. Three replicates were performed for each competition. (B) Competition assays in *pkr* +/+ MEFs. (C) Correlation between fitness in *pkr* −/− and *pkr* +/+ cells. Error bars represent the standard error of the mean

effects were confirmed for mutants G2686A ($W = 2.18$; $P = 0.047$), G3351A ($W = 22.9$; $P = 0.008$), and A3460C ($W = 8.46$; $P = 0.025$), whereas A8679C and A11090G did not deviate significantly from neutrality ($P \geq 0.08$; Fig. 3A). Interestingly, the G3837A mutation also had a negative fitness impact on *pkr* −/− MEFs ($W = 0.254$; $P = 0.031$). The fact that this mutation was deleterious regardless of cell type (BHK-21, *pkr* +/+ MEFS, or *pkr* −/− MEFs) but appeared in four out of five evolved lines indicates strong sign epistasis. However, these genetic interactions were probably complex, since the G3837A change did not occur in systematic association with any other substitution (Table 2).

We then performed competition assays of the single mutants in *pkr* +/+ MEFs to determine whether their effects were PKR specific. However, we again found increased fitness for mutants G2686A ($W = 6.00$; $P = 0.006$), G3351A ($W = 5.06$; $P = 0.050$), and A3460C ($W = 3.11$; $P = 0.041$), thus indicating that these were generally beneficial mutations in MEFs regardless of PKR status. Also reproducing the results obtained in *pkr* −/− cells, A8679C and A11090G were apparently neutral ($P \geq 0.19$; Fig. 3B). Therefore, the hypothesis of an adaptive trade-off whereby the effects of these mutations in *pkr* +/+ and *pkr* −/− cells would be negatively correlated was not supported (Pearson $r = 0.737$; $P = 0.059$; Fig. 3C). We, therefore, conclude that PKR-specific adaptation was determined by other, non-parallel, mutations or a combination of mutations showing epistasis.

4 Discussion

We found a large number of parallel sequence changes in the five evolved lines, similar to previous work (Cuevas, Elena, and Moya 2002; Novella et al. 2004, 2010; Remold, Rambaut, and Turner 2008; Cuevas, Moya, and Sanjuán 2009). To further assess whether these changes were cell type -specific, host species-specific, or generally beneficial mutations under laboratory conditions, we reviewed sequences from previous experiments in which VSV was adapted to MEFs, BHK-21 cells, human cervix cancer HeLa cells, and dog kidney MDCK cells. We found that the G2686A substitution appeared in two of four lines evolved in HeLa cells (Remold, Rambaut, and Turner 2008), whereas the A3460C mutation appeared in one line evolved in BHK-21 cells (Novella et al. 2004) and in one line evolved in p53-deficient MEFs (Garijo et al. 2014). Strikingly, the highly deleterious mutation G3837A appeared in five lines evolved in BHK-21 cells (Novella et al. 2010) and in three out of five lines evolved in MDCK cells (Cuevas, Moya, and Sanjuán 2009). The C10224U mutation, which we failed to rescue, was found in one line evolved in p53 knock-out MEFs (Garijo et al. 2014). Additionally, the C4180A mutation, which appeared only once in *pkr* −/− MEFs was found in more than ten lines evolved in BHK-21 cells (Novella et al. 2010) and in one of four lines evolved in HeLa cells (Remold, Rambaut, and Turner 2008). Finally, although we did not find the G3351A mutation reported in previous works, it appeared under our laboratory conditions after serial transfers in BHK-21 cells (unpublished data). Therefore, most parallel substitutions probably correspond to generally beneficial mutations conferring adaptation to cell culture conditions. This is particularly likely considering that, in our experiments, the founder virus was recovered from an infectious cDNA clone with no previous laboratory passaging history. A candidate factor that is common to all the above cell lines is immortalization, which often tends to constitute a permissive environment for viruses. The various parallel mutations found in the glycoprotein G may also improve viral attachment/entry in mammalian fibroblasts such as BHK-21, MEF, or MDCK cells, which are not the natural target cell type of VSV.

All parallel changes were non-synonymous except for A11090G, which mapped to the trailer sequence. To explore possible effects of this mutation, we obtained the predicted minimum free energy secondary structure of the trailer sequence using the RNAfold program (Gruber et al. 2008). This gave a highly folded structure, with 66 out of 100 sites forming intramolecular base pairs (Fig. 4). The A11090G mutation mapped to position 28 of the trailer and introduced a new base pair which displaced the next 12 bases, thus producing a major change in the predicted structure. The leader and trailer are the only VSV transcripts which are not 5'-capped and have a 5ppp terminus (Gerlier and Lyles 2011). This type of RNA can be a RIG-I agonist provided that it contains dsRNA regions formed by intramolecular base pairs, triggering interferon secretion and an innate immune response. Furthermore, partially double-stranded 5ppp RNA can directly activate PKR in an interferon-dependent manner (Nallagatla et al. 2007), leading to EI2F alpha phosphorylation and translation arrest. This suggests that slight changes in RIG-I induction may be tolerated in the absence of a major antiviral effector such as PKR but not in normal cells. However, as shown above, the A11090G single mutant did not experience

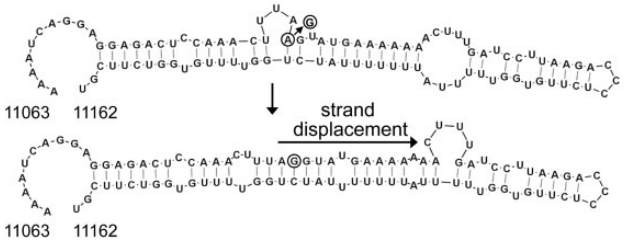

Figure 4. Effect of the A11090G mutation on the predicted secondary structure of the trailer. The minimum free energy (MFE) structure predicted by the RNAfold program is shown for the T0 (top) and A11090G (bottom) trailers. Numbers indicate genome positions. The mutated base is circled. In the predicted MFE structure, the single-base substitution modified 14 neighboring base pairs, as indicated

fitness defects in *pkr* −/− or *pkr* +/+ MEFs. It is possible though that PKR-specific fitness effects may arise from epistatic interactions between A11090G and other mutations. Interestingly, the A11090G, A8679C, and G2686A changes co-occurred in lines L2 and L5, suggesting that they may be an epistatic set. This speculation is substantiated by the fact that G2686A produced a non-conservative (G146E) amino acid replacement in protein M, which is the only VSV protein known to block innate immunity (Faul, Lyles, and Schnell 2009; Rieder and Conzelmann 2009).

In conclusion, our results show that serial transfers in cells with a specific genetic defect in innate immunity do not produce an easily identifiable, repeatable change in viral sequence which could be used for engineering an attenuated virus. Parallel substitutions occurred, but these were generally beneficial and thus were not responsible for *pkr*-specific changes in fitness. These changes should thus be driven by singleton substitutions, which may sometimes act epistatically. Although the majority of these substitutions were synonymous, they may still have fitness effects, which remain to be characterized. In contrast to directed evolution experiments showing deterministic changes at the molecular level, we suggest that the fixation of mutations under relaxed selection is governed by random genetic drift. These types of mutations would be tolerated under the permissive environment but not in cells with intact antiviral responses, thus driving viral specialization and attenuation. However, the stochastic nature of molecular evolution and epistasis make it inherently difficult to use a relaxed selection approach for the rational, molecularly informed attenuation of viruses, a desirable goal in the clinical setting.

Acknowledgements

We thank Silvia Torres for technical assistance and Dr Carmen Rivas for the *pkr*−/− MEFs. This work was supported by grants from the Spanish MINECO (BFU2013-41329) and the European Research Council (ERC-2011-StG-281191-VIRMUT) to R.S.

Data availability

All data are available upon request.

Conflict of interest: None declared.

References

Agudelo-Romero, P., de la Iglesia F., and Elena S. F. (2008) 'The Pleiotropic Cost of Host-Specialization in Tobacco Etch Potyvirus', *Infection, Genetics and Evolution*, 8: 806–14.

Balachandran, S. et al. (2000) 'Essential Role for the dsRNA-Dependent Protein Kinase PKR in Innate Immunity to Viral Infection', *Immunity*, 13: 129–41.

Betancourt, A. J. (2009) 'Genomewide Patterns of Substitution in Adaptively Evolving Populations of the RNA Bacteriophage MS2', *Genetics*, 181: 1535–44.

Borderia, A. V. et al. (2015) 'Group Selection and Contribution of Minority Variants during Virus Adaptation Determines Virus Fitness and Phenotype', *PLoS Pathogens*, 11: e1004838.

Bowie, A. G., and Unterholzner L. (2008) 'Viral Evasion and Subversion of Pattern-Recognition Receptor Signalling', *Nature Reviews Immunology*, 8: 911–22.

Buckling, A. et al. (2009) 'The Beagle in a Bottle', *Nature*, 457: 824–9.

Cahn, P., and Wainberg M. A. (2010) 'Resistance Profile of the New Nucleoside Reverse Transcriptase Inhibitor Apricitabine', *Journal of Antimicrobial Chemotherapy*, 65: 213–7.

Chao, L. (1990) 'Fitness of RNA Virus Decreased by Muller's Ratchet', *Nature*, 348: 454–5.

Ciota, A. T. et al. (2014) 'Consequences of In Vitro Host Shift for St. Louis Encephalitis Virus', *Journal of General Virology*, 95: 1281–8.

Coffey, L. L., and Vignuzzi M. (2011) 'Host Alternation of Chikungunya Virus Increases Fitness While Restricting Population Diversity and Adaptability to Novel Selective Pressures', *Journal of Virology*, 85: 1025–35.

Cuevas, J. M., Elena S. F., and Moya A. (2002) 'Molecular Basis of Adaptive Convergence in Experimental Populations of RNA Viruses', *Genetics*, 162: 533–42.

——, Moya A., and Sanjuán R. (2005) 'Following the Very Initial Growth of Biological RNA Viral Clones', *Journal of General Virology*, 86: 435–43.

——, ——, and ——. (2009) 'A Genetic Background with Low Mutational Robustness is Associated with Increased Adaptability to a Novel Host in an RNA Virus', *Journal of Evolutionary Biology*, 22: 2041–8.

Cunningham, C. W. et al. (1997) 'Parallel Molecular Evolution of Deletions and Nonsense Mutations in Bacteriophage T7', *Molecular Biology and Evolution*, 14: 113–6.

Dabo, S., and Meurs E. F. (2012) 'dsRNA-Dependent Protein Kinase PKR and Its Role in Stress, Signaling and HCV Infection', *Viruses*, 4: 2598–635.

de la Iglesia, F., and Elena S. F. (2007) 'Fitness Declines in Tobacco Etch Virus upon Serial Bottleneck Transfers', *Journal of Virology*, 81: 4941–7.

Duarte, E. et al. (1992) 'Rapid Fitness Losses in Mammalian RNA Virus Clones due to Muller's Ratchet', *Proceedings of the National Academy of Science United States of America*, 89: 6015–9.

Duffy, S., Turner P. E., and Burch C. L. (2006) 'Pleiotropic Costs of Niche Expansion in the RNA Bacteriophage Phi 6', *Genetics*, 172: 751–7.

Faul, E. J., Lyles D. S., and Schnell M. J. (2009) 'Interferon Response and Viral Evasion by Members of the Family Rhabdoviridae', *Viruses*, 1: 832–51.

García, M. A., Meurs E. F., and Esteban M. (2007) 'The dsRNA Protein Kinase PKR: Virus and Cell Control', *Biochimie*, 89: 799–811.

Garijo, R. et al. (2014) 'Experimental Evolution of an Oncolytic Vesicular Stomatitis Virus with Increased Selectivity for p53-Deficient Cells', *PLoS One*, 9: e102365.

Gerlier, D., and Lyles D. S. (2011) 'Interplay between Innate Immunity and Negative-Strand RNA Viruses: Towards a Rational Model', *Microbiology and Molecular Biology Reviews*, 75: 468–90.

Gruber, A. R. et al. (2008) 'The Vienna RNA Websuite', *Nucleic Acids Research*, 36: W70–4.

Hoffmann, H. H., Schneider W. M., and Rice C. M. (2015) 'Interferons and Viruses: An Evolutionary Arms Race of Molecular Interactions', *Trends in Immunology*, 36: 124–38.

Koev, G., and Kati W. (2008) 'The Emerging Field of HCV Drug Resistance', *Expert Opinion on Investigational Drugs*, 17: 303–19.

Martin, J., and Minor P. D. (2002) 'Characterization of CHAT and Cox Type 1 Live-Attenuated Poliovirus Vaccine Strains', *Journal of Virology*, 76: 5339–49.

Minor, P. D. (2015) 'Live Attenuated Vaccines: Historical Successes and Current Challenges', *Virology*, 479–480C: 379–92.

Miralles, R., Moya A., and Elena S. F. (2000) 'Diminishing Returns of Population Size in the Rate of RNA Virus Adaptation', *Journal of Virology*, 74: 3566–71.

Munir, M., and Berg M. (2013) 'The Multiple Faces of Proteinkinase R in Antiviral Defense', *Virulence*, 4: 85–9.

Nallagatla, S. R. et al. (2007) '5'-Triphosphate-Dependent Activation of PKR by RNAs with Short Stem-Loops', *Science*, 318: 1455–8.

Novella, I. S., and Ebendick-Corpus B. E. (2004) 'Molecular Basis of Fitness Loss and Fitness Recovery in Vesicular Stomatitis Virus', *Journal of Molecular Biology*, 342: 1423–30.

——, Zárate S., Metzgar D., and Ebendick-Corpus B. E.et al. (2004) 'Positive Selection of Synonymous Mutations in Vesicular Stomatitis Virus', *Journal of Molecular Biology*, 342: 1415–21.

——, and Ebendick-Corpus B. E. et al. (2010) 'Genomic Evolution of Vesicular Stomatitis Virus Strains with Differences in Adaptability', *Journal of Virology*, 84: 4960–8.

Palmero, I., and Serrano M. (2001) 'Induction of Senescence by Oncogenic Ras', *Methods in Enzymology*, 333: 247–56.

Pindel, A., and Sadler A. (2011) 'The Role of Protein Kinase R in the Interferon response', *Journal of Interferon and Cytokine Research*, 31: 59–70.

Remold, S. K., Rambaut A., and Turner P. E. (2008) 'Evolutionary Genomics of Host Adaptation in Vesicular Stomatitis Virus', *Molecular Biology and Evolution*, 25: 1138–47.

Rico, P., et al. (2006) 'Insights into the Selective Pressures Restricting Pelargonium Flower Break Virus Genome Variability: Evidence for Host Adaptation', *Journal of Virology*, 80: 8124–32.

Rieder, M., and Conzelmann K. K. (2009) 'Rhabdovirus Evasion of the Interferon System', *Journal of Interferon and Cytokine Research*, 29: 499–509.

Robinson, M. et al. (2011) 'Preexisting Drug-Resistance Mutations Reveal Unique Barriers to Resistance for Distinct Antivirals', *Proceedings of the National Academy of Science United States of America*, 108: 10290–5.

Sanjuán, R., Moya A., and Elena S. F. (2004) 'The Distribution of Fitness Effects Caused by Single-Nucleotide Substitutions in an RNA Virus', *Proceedings of the National Academy of Science United States of America*, 101: 8396–401.

Stojdl, D. F. et al. (2000) 'The Murine Double-Stranded RNA-Dependent Protein Kinase PKR is Required for Resistance to Vesicular Stomatitis Virus', *Journal of Virology*, 74: 9580–5.

Triana-Baltzer, G. B. et al. (2011) 'Phenotypic and Genotypic Characterization of Influenza Virus Mutants Selected with the Sialidase Fusion Protein DAS181', *Journal of Antimicrobial Chemotherapy*, 66: 15–28.

Turner, P. E., and Elena S. F. (2000) 'Cost of Host Radiation in an RNA Virus', *Genetics*, 156: 1465–70.

——, and —— et al. (2010) 'Role of Evolved Host Breadth in the Initial Emergence of an RNA virus', *Evolution*, 64: 3273–86.

Versteeg, G. A., and Garcia-Sastre A. (2010) 'Viral Tricks to Grid-Lock the Type I Interferon System', *Current Opinion in Microbiology*, 13: 508–16.

Wainberg, M. A., Mesplede T., and Quashie P. K. (2012) 'The Development of Novel HIV Integrase Inhibitors and the Problem of Drug Resistance', *Current Opinion in Microbiology*, 2: 656–62.

Whelan, S. P. et al. (1995) 'Efficient Recovery of Infectious Vesicular Stomatitis Virus Entirely from cDNA Clones', *Proceedings of the National Academy of Science United States of America*, 92: 8388–92.

Wichman, H. A., and Brown C. J. (2010) 'Experimental Evolution of Viruses: Microviridae as a Model System', *Philosophical Transactions of the Royal Society of London B Biological Sciences*, 365: 2495–501.